Structure and function of a YeeE-YeeD complex for sophisticated thiosulfate uptake

Authors

Mai Ikei[1,†], Ryoji Miyazaki[1,†], Keigo Monden[1], Yusuke Naito[1], Azusa Takeuchi[1], Yutaro S. Takahashi[1], Yoshiki Tanaka[1], Takaharu Mori[2], Muneyoshi Ichikawa[3,*], Tomoya Tsukazaki[1,*]

Affiliations

[1]Division of Biological Science, Graduate School of Science and Technology, Nara Institute of Science and Technology, Ikoma, Nara 630-0192, Japan.

[2]Department of Chemistry, Faculty of Science, Tokyo University of Science, Shinjuku-ku, Tokyo 162-8601, Japan

[3]State Key Laboratory of Genetic Engineering, Department of Biochemistry and Biophysics, School of Life Sciences, Fudan University, Shanghai 200438, China.

[*]Corresponding author. Email: ichikawa_muneyoshi@fudan.edu.cn (M. Ichikawa); ttsukaza@bs.naist.jp (T.T.)

[†]These authors contributed equally to this work.

Abstract

Uptake of thiosulfate ions as an inorganic sulfur source from the environment is important for bacterial sulfur assimilation. Recently, a selective thiosulfate uptake pathway involving membrane protein YeeE (TsuA) was characterized. However, the precise function of YeeE and a putative cofactor in the thiosulfate ion uptake pathway remained unclear. Here, we assessed selective thiosulfate transport via YeeE in vitro and characterized YeeD (TsuB) as an adjacent and essential cofactor for YeeE-mediated thiosulfate uptake in vivo. We further showed that YeeD possesses thiosulfate decomposition activity and that a conserved cysteine in YeeD was modified in several forms in the presence of thiosulfate. Finally, the crystal structure of a YeeE-YeeD fusion protein at 2.6-Å resolution revealed their interactions. The association was evaluated by a binding assay using purified proteins. Based on these results, a model of the sophisticated uptake of thiosulfate ions by YeeE and YeeD is proposed.

INTRODUCTION

From bacteria to eukaryotes, sulfur is a vital element for cellular activities. For example, sulfur-containing biomolecules, such as L-cysteine, L-methionine, thiamine, glutathione, and biotin, play a variety of essential roles in cells (*1*). Bacteria and plants can utilize L-cysteine as a source of sulfate, but they also have sulfur assimilation pathways to synthesize L-cysteine from inorganic sulfur compounds. In bacteria, L-cysteine is important not only as a component for protein synthesis but also as a reducing agent against oxidative stress (*2*). There are two pathways for bacterial L-cysteine synthesis, which use O-acetylserine as a precursor, called the sulfate and thiosulfate pathways (*3*). In the sulfate pathway, sulfate ion is first decomposed into sulfide ion through phosphorylation by two molecules of ATP and reduction by four molecules of NADPH. Subsequently, L-cysteine is synthesized from sulfide ion and O-acetylserine by O-acetylserine sulfhydrylase-A (CysK). In the thiosulfate pathway, S-sulfocysteine is synthesized from thiosulfate ion and O-acetylserine by O-acetylserine sulfhydrylase-B (CysM); S-sulfocysteine is then reduced by one NADPH molecule, and L-cysteine is synthesized. The sulfate and thiosulfate ions used in these pathways are taken up from the environment by transporters on the cytoplasmic membrane. Sulfate and thiosulfate ions are trapped by periplasmic proteins Sbp (*4*) and CysP (*5*), respectively. Both sulfate and thiosulfate ions are then passed on to a complex formed by the inner membrane proteins CysU and CysW and the cytosolic protein CysA (CysUWA) (also called CysTWA) (*3*) and transported into the cytoplasm by the CysUWA complex using the energy from ATP hydrolysis.

A bacterial membrane protein, YeeE, has been identified as mediating thiosulfate uptake based on growth complementation assay of *Escherichia coli* cells, and the structure of *Spirochaeta thermophila* YeeE (*St*YeeE) has been determined by X-ray crystallography (*6*). YeeE was proposed to be almost entirely buried in the membrane and shows a unique hourglass-like structure. An electron density near a conserved cysteine residue on the outside surface was assigned to a thiosulfate ion. In addition, the binding of thiosulfate ions to purified YeeE protein was shown by isothermal titration calorimetry experiments. In the center of YeeE, three conserved, functionally important cysteines, including the thiosulfate-interacting one, are arranged side by side and perpendicular to the membrane. Based on these structural features and in vivo functional analysis using a series of mutants, thiosulfate ion was proposed to be transported from the environment to the cytoplasm while transiently interacting with three conserved cysteine residues, independently of the thiosulfate pathway described above. However, it has not been elucidated whether YeeE alone transports thiosulfate ions. Moreover, no YeeE cofactor has been clearly defined, although one candidate gene is *yeeD*, which resides within the same operon that includes *yeeE* (*7*), and the regulatory mechanism of the alternative, sophisticated

thiosulfate uptake by YeeE remains unclear.

Recently, in addition to the *yeeE* gene, *yeeD* was shown to be involved in thiosulfate uptake and the two were named *tsuA* and *tsuB*, respectively (*8*). YeeD is a cytoplasmic protein that belongs to the TusA (tRNA 2-thiouridine synthesizing protein A) protein family (*9*). TusA plays various roles in sulfate transfer activities in cells, such as thiomodification of tRNA (*10*), molybdenum cofactor biosynthesis (*11*), and dissimilatory sulfur and tetrathionate oxidation (*12*). The cysteine residue in a Cys-Pro-X-Pro (CPxP) motif of TusA receives activated sulfur from the L-cysteine desulfurase IscS (*13*). Although YeeD possesses the CPxP motif, it cannot complement TusA function (*11*). Therefore, YeeD is thought to have a sulfate-related yet distinct function from TusA in bacteria. In some bacteria, such as Gram-positive *Corynebacterium*, YeeE and YeeD are expressed as one polypeptide, implying that YeeD works as a cofactor of YeeE in the thiosulfate uptake pathway. However, the enzymatic activity of YeeD and the functional cooperativity of YeeE and YeeD have not been well characterized.

In this study, first, we measured thiosulfate uptake activity using YeeE-reconstituted liposomes to clarify YeeE function. Second, according to a growth complementation assay, we found that YeeD plays an essential role in YeeE function in vivo. Third, we demonstrated a thiosulfate decomposition activity in purified YeeD. Fourth, direct interaction between YeeE and YeeD proteins was detected, and substrate thiosulfate ions weakened the binding of these proteins. Fifth, the crystal structure of the YeeE–YeeD complex was determined at 2.60-Å resolution. Critical residues of YeeD for both its activity and interaction with YeeE were defined. Based on these results, detailed mechanisms for the functional cooperation between YeeE and YeeD in thiosulfate uptake are proposed.

RESULTS

YeeE-mediated thiosulfate transport

Although *E. coli* growth complementation tests showed that YeeE is involved in the uptake of thiosulfate ions (*6*), thiosulfate transport via YeeE has not yet been demonstrated. To detect thiosulfate uptake activity using a purified reconstituted system, we adapted solid-supported membrane (SSM)-based electrophysiology (*14*). First, *St*YeeE-reconstituted liposomes were applied to the SSM, and charge displacement was measured in the presence of sulfate ions or thiosulfate ions (Fig. 1A). A change in the potential toward the negative direction was observed in the presence of thiosulfate ions but not sulfate ions, meaning that negatively charged thiosulfate ions were selectively transported into the proteoliposomes. The slight change in the potential toward the positive direction in the presence of sulfate ions was probably due to buffer shock since there was no counter ion present in these measurements. Next, because *St*YeeE-reconstituted liposomes showed no transport activity for sulfate ions, we measured YeeE activity using sulfate as a counter ion. As a result, a clear peak toward the negative direction (-0.62 nA) was observed only in the presence of *St*YeeE (Fig. 1B). The negative peak area increased when higher concentrations of thiosulfate ions were used (Fig. 1C). These experiments verified that YeeE transports thiosulfate ions specifically but not sulfate ions.

YeeD is essential for the YeeE-mediated thiosulfate pathway

According to recent reports (*7, 8*), YeeD may function in combination with YeeE in vivo. YeeD is composed of about 80 amino acid residues and possesses one or two cysteines, which are highly conserved among bacteria. In some organisms, such as *E. coli*, YeeD has two conserved cysteine residues (C13 and C39 in *E. coli* YeeD (*Ec*YeeD)), while other organisms like *S. thermophila* have one conserved cysteine residue (C17 in *St*YeeD) (Fig. 2A). The invariant cysteine residue in the N-terminal region is part of a CPxP motif that is conserved among TusA family proteins (Fig. 2A and fig. S1). The predicted *Ec*YeeD structure in the AlphaFold2 database (*15, 16*) shows a globular shape with two α-helices and a β-sheet composed of four β-strands (Fig. 2B), similar to other TusA protein structures (*17, 18*). To evaluate the influence of Yeed on YeeE activity in cells, a growth complementation assay using *E. coli* MG1655 *ΔcysPUWA ΔyeeE::kan* (DE3) cells was performed, as described previously (*6*). These *E. coli* cells, which lack sulfate and thiosulfate ion-uptake pathways, cannot grow in the presence of thiosulfate as a sole sulfur source (Fig. 2C and fig. S2, A and B), but can when they carry a plasmid containing the *E. coli yeeE* operon, which includes *yeeE* and *yeeD* (*6*) (Fig. 2C). When the *yeeD* region was deleted, growth was similar to the negative control (Fig. 2C), revealing that YeeD is essential for thiosulfate uptake via YeeE in vivo. Further, we identified the

critical residues C13 and C39 of *Ec*YeeD in the growth complementation assay using several YeeD mutants (Fig. 2C).

Thiosulfate decomposition activity of YeeD and its catalytic center residue

To unveil the enzymatic function of YeeD itself, we used purified *St*YeeD. Purified *St*YeeD(WT) in an SDS-PAGE gel exhibited a main band and a minor upshifted band, whereas *St*YeeD(C17A), a putative catalytic center mutant, exhibited only the main band (Fig. 2, D and E). A similar band shift was reported for purified *Pseudomonas aeruginosa* PA1006, an ortholog of *E. coli* TusA (*19*). PA1006 has one conserved cysteine residue corresponding to C17 of *St*YeeD, and the cysteine side chain of PA1006 was shown to be persulfide-modified by mass spectrometry (MS). To examine *St*YeeD modification at C17, we performed a matrix-assisted laser desorption ionization-time of flight (MALDI-TOF) MS in the absence of thiosulfate (Fig. 2D), which revealed three major peaks with m/z of 11316.1, 11348.8, and 11393.5. The first peak (11316.1 m/z) was assigned as unmodified *St*YeeD (-SH at C17) as its theoretical m/z value is 11315.7. The second peak (11348.8 m/z) might correspond to sulfinic acid (-S-O_2^- at C17) as it increased by 32.7 (close to the value of 2 oxygen atoms, 32.0) though it is also possible that a peak of persulfide modification (-S-S^- at C17) overlaps. The third 77.4 m/z-increased peak (11393.5 m/z) may be attributable to sulfonate (-S-SO_3^- at C17). In contrast, *St*YeeD(C17A) showed only one prominent peak (11283.5 m/z) as its theoretical unmodified value (11283.6 m/z) (Fig. 2E). These results suggest that the C17 of *St*YeeD is highly reactive to sulfur-related molecules and susceptible to sulfur-related modifications. Next, to identify the second peak, we performed MS analysis of the *St*YeeD protein in the presence of DL-Dithiothreitol (DTT), a reductant. The third peak entirely disappeared after the addition of DTT (Fig. 2F). By contrast, the second peak remained even in the presence of DTT. Persulfide modification (-S-S^-) can be reduced by DTT (*19*) but sulfinic acid (-S-O_2^-), an overoxidation product, is irreversible as previously shown (*20*). Therefore, the second peak was assigned as a sulfinic acid product though we cannot exclude the possibility of a slight presence of the persulfide modification product. Finally, to gain insights into catalytic intermediates, MS analysis was performed in the presence of thiosulfate (Fig. 2G). In the condition with thiosulfate, a peak with m/z value of 11428.6 appeared. This may correspond to -S-$S_2O_3^-$ because the m/z increments were equivalent to the addition of S_2O_3 to StYeeD(-SH). In the case of StYeeD(C17A), the addition of thiosulfate did not increase the m/z (fig. S2C).

The additional binding of S_2O_3 to the C17 side chain, in form of -S-$S_2O_3^-$, and the existence of sulfonate (-S-SO_3^- at C17), as indicated by the MS results, raise the possibility that YeeD decomposes thiosulfate ion ($S_2O_3^{2-}$) and releases sulfide ion (S^{2-}). To test this, we monitored hydrogen

sulfide (H_2S) derived from thiosulfate-decomposed sulfide ions using a fluorescent probe for H_2S, HSip-1. A significant increase in fluorescence intensity was observed in the presence of *St*YeeD compared with an irrelevant protein, BSA, and with no protein (Fig. 2H and fig. S2D), suggesting that YeeD catalyzes the decomposition of thiosulfate as a substrate. We also tested the thiosulfate decomposition activity of several *St*YeeD mutants. Among these, only C17A did not show a significant increase in fluorescence. These results indicated that the conserved cysteine residue of YeeD (C17 in *St*YeeD) is the catalytic center residue for thiosulfate decomposition.

Crystal structure of the YeeE-YeeD complex

We determined the crystal structures of the *St*YeeE-YeeD complex at 3.34-Å and 2.60-Å resolution (Fig. 3A and Table 1), which enables us to discuss the detailed interactions between YeeE and YeeD. The crystallized sample was a fusion protein of *St*YeeE and *St*YeeD, designed based on the amino acid sequence of *Corynebacterium pollutisoli* YeeED, which is expressed as a single protein. The forty amino acid residues that connect the C-terminus of *St*YeeE and the N-terminus of *St*YeeD were structurally disordered. Crystals were also successfully obtained after introducing the C22A mutation into YeeE (Table 1 8J4C). The higher resolution structure was solved by introducing an additional stable mutation, L45A in YeeD (as described later) (Table 1 8K1R). Each crystal lattice in the datasets was the same, except for having slightly different unit cell dimensions. The asymmetric unit contains two molecules of StYeeED, Mol A and Mol B. In the crystal packing, YeeD in Mol A is involved in interacting with an adjacent YeeD region, but YeeD in Mol B is not. When the two YeeE-YeeD structures (Mol A and Mol B), showing different packing interactions, were superimposed, the crystal structures were almost identical with an RSMD of 0.433 Å for 8J4C or 0.155 Å for 8K1R for Cα atoms (fig. S3, A and B). Although the orientation of YeeD relative to YeeE is slightly different, the RMSD between 8J4C and 8K1R for Cα atoms is 0.896 (fig. S3C) and the active site of YeeD is similar. Therefore, in this paper, we introduce Mol A of the higher resolution structure, which shows the best electron density map, to explain YeeE and YeeD interactions.

The overall structure of YeeE in the crystal structure of YeeE-YeeD resembles the previously reported crystal structure of YeeE (*6*), with an RMSD of 0.596 Å for Cα atoms (fig. S3D). The cytoplasmic indentation of YeeE associates with YeeD, which consists of two α-helices and four β-sheets. The architecture of YeeD is similar in shape to the sequence-homologous TusA (22.5% identical) (fig. S3E). Residues involved in the YeeE-YeeD interaction are shown in Fig. 3B. C22 of YeeE is located at the interface, implying that C22A affects the interaction. Residues R28, R98, E101, and E261 on the cytoplasmic surface, conserved in YeeEs (*6*), were found to be involved in the

interaction with YeeD. While the important, conserved residues C293, C91, and C22, termed the first, second, and third cysteines, respectively, are arranged perpendicular to the membrane at 8.6- and 6.7-Å intervals, C17 of YeeD, one of the YeeE-interacting residues, is the putative enzymatic active site and is located adjacent to C22 of YeeE as the "fourth cysteine". This positioning means that a thiosulfate ion transported through the membrane via the center region of YeeE interacts with the first-to-third cysteines of YeeE in succession and then interacts with the fourth cysteine of YeeD. The distance between the third and the fourth cysteines, 10.8 Å, is wider than that between the other cysteines, and this space may be needed for transient binding of the thiosulfate ion rather than its transport (Fig. 3C). A water molecule is located at position III, a predicted thiosulfate-binding site (6). A position where another water molecule is located below position III corresponds to the position of the side chain of C22 (6). The relay of a thiosulfate ion from position III to C17 is likely facilitated by the conserved positively charged residues R28 and R98 (Fig. 3C). The CPxP motif forms a cis peptide between C17 and P18 and is located at the beginning of the α-alpha helix (Fig. 3D), similar to a previous report (*17*). In addition, the electron density of the peptide bonds between V16 and C17 is faint, which may be closely related to C17 being the active center.

Interaction between YeeE and YeeD.

To confirm that the interactions between YeeE and YeeD revealed in the crystal structure of the YeeE-YeeD fusion protein also occur in solution, we performed a binding assay based on the bio-layer interferometry (BLI) method (*21*) using purified *St*YeeE and His-tagged *St*YeeD. Clear association and dissociation of *St*YeeE with an *St*YeeD-solidified Ni-NTA sensor were observed as real-time wavelength shifts (Fig. 4A, blue). Based on the YeeE binding-dependent wavelength changes, the K_D between *St*YeeD and *St*YeeE was estimated as 1.35 ± 0.13 μM. When a buffer containing sulfate ion was used, the binding was similar to that in a buffer without a sulfur source (fig. S4, A and B). In contrast, YeeE showed significantly decreased binding to YeeD in a buffer containing thiosulfate ions (fig. S4, A and B). We next sought the important residues for the interaction using a series of *St*YeeD mutants. The mutants E15A, V16A, C17A, D42A, Y43A, E48A, and R49A severely impaired *St*YeeD's affinity for *St*YeeE, while the mutant L45A enhanced the affinity (Fig. 4B). This enhanced affinity could stabilize the crystal packing of YeeE-YeeD, leading to its higher resolution structure. In the crystal structure, most of these influential residues for affinity were located at the border region between YeeE and YeeD (Fig. 4C). On the other hand, Ala substitutions on the opposite side maintained affinity (Fig. 4). Notably, the conserved cysteine residue (C17) of *St*YeeD proved to be pivotal for not only the enzyme activity but also the interaction with *St*YeeE. These BLI results in

solution are consistent with the crystal structure.

To further assess the important residues of YeeE for the interaction with YeeD, we used a growth complementation assay. *Ec*YeeE mutations of residues at the interaction surface (R21A, R101A, E104A, E271A, R275A) could not complement the growth of *E. coli* MG1655 *ΔcysPUWA ΔyeeE::kan* (DE3) cells (fig. S4, C and D). These results emphasize that the interaction of YeeE and YeeD is essential for in vivo function of thiosulfate uptake.

DISCUSSION

By the growth complementation assay, we have demonstrated that YeeD is essential for the activity of YeeE in vivo. YeeD's substrate was identified as the thiosulfate ion, and the uptake activity for thiosulfate ions was measured using YeeE-reconstituted liposomes. In addition, the interaction between YeeE and YeeD was revealed by both binding assay and X-ray crystallography. By mutational analysis of YeeD, a conserved cysteine residue was found to be critical for YeeE's activity in vivo as well as thiosulfate ion decomposition activity.

Based on our findings, we propose detailed mechanisms for thiosulfate ion uptake by YeeE and YeeD (Fig. 5A). From the previous crystal structure of *St*YeeE, the transportation of thiosulfate ions across the membrane was proposed to be relayed by the first-to-third cysteine residues (*6*). Our crystal structure of YeeE and YeeD complex now further shows that YeeD is positioned to interact with the YeeE cytoplasmic side, which we propose to be the exit of the thiosulfate pathway on YeeE; the conserved cysteine residue of YeeD can function as a "fourth cysteine". Therefore, the interactions between the two can facilitate the delivery of a thiosulfate ion from YeeE to YeeD: the conserved cysteine residue of YeeD can directly capture a thiosulfate ion passed through YeeE, resulting in thiosulfonated YeeD. Our BLI method analysis in the presence of thiosulfate showed that the interaction between YeeD and YeeE was weakened, possibly due to thiosulfonation on YeeD. The thiosulfonated YeeD may therefore dissociate from YeeE and be released to the cytoplasm. Since YeeD can decompose thiosulfate by itself, the YeeD would decompose thiosulfate after dissociating from YeeE.

We suggest a plausible mechanism for decomposition of thiosulfate ion by YeeD (Fig. 5B). In the presence of thiosulfate ion, YeeD incorporated thiosulfate, but YeeD(C17A) did not (Fig. 2F and fig. S2C), suggesting that the thiosulfate ion directly binds to the cysteine residue of YeeD. Taking this together with the detection of H_2S in the presence of YeeD and thiosulfate ion (Fig. 2H), we propose that sulfide ion (S^{2-}) is released from thiosulfonated YeeD; after this, sulfite ion (SO_3^{2-}) is released, and the cycle is repeated (Fig. 5B). In the 2.60-A structure of YeeE-YeeD, the electron density

is faint in the N-terminal side of the CPxP motif, raising the possibility that some electrons may be attracted to the CPxP motif (Fig. 3D). If that happens, forming the CPxP motif could make the region electron-rich and exhibit high reducing power. Previously, the CPxP architecture was proposed to stabilize an α-helix-1 by capping it (*17*). In the TusA family proteins, the formation of CPxP may also provide high reducing power, exhibiting the unique property of selective decomposition of their substrates.

Compared with other TusA family proteins, YeeD shows several distinct characteristics. Although conserved cysteine residues in other TusA family proteins, corresponding to C17 in *St*YeeD, are important for their own activities (*10, 19*), TusA could not decompose thiosulfate ions (*22*). The conserved cysteine residues in YeeD and TusA are important for binding to their respective partners (Fig. 4) (*12, 18*), which seems to be a common feature in TusA family proteins. Meanwhile, YeeD is unique in that its interaction partner, YeeE, is a membrane protein, unlike other TusA family proteins. In addition, YeeD differs from other members of the TsuA family in terms of modifications to conserved cysteines. Previously, the conserved cysteine residue of PA1006 was reported to be persulfide-modified (*19*). In contrast, YeeD has several different sulfur-related modification statuses, including sulfonate and thiosulfonate (Fig. 2, D, F, and G). In the case of DsrE3 and TusA, the conserved cysteines can possess thiosulfonate, but the modifications were detected only with their substrate tetrathionate (*12*). Along with the fact that YeeE only allows thiosulfate to pass through, YeeD also seems to be specialized for thiosulfate reactivity. Both can contribute to the efficient uptake of thiosulfate. Since YeeE alone can transport thiosulfate ions but was unable to rescue the growth deficiency in vivo, cooperation between YeeE and YeeD is crucial. In this study, we have unveiled a sophisticated pathway for thiosulfate uptake in the bacterial membrane. An open question is whether there are other proteins that directly receive sulfur compounds from YeeD in sulfur assimilation pathways.

In conclusion, we revealed that YeeE and YeeD cooperatively contribute to the thiosulfate uptake pathway and possess unprecedented regulation mechanisms. Our findings also deepen the understanding of the functions of TusA family proteins.

MATERIALS AND METHODS

Strains and plasmids

For the growth complementation assay, we used plasmids derived from pAZ061, which is based on pET-16b-TEV (*23*) and possesses *E. coli yeeE* and *yeeD* genes between BamHI and XhoI sites amplified from *E. coli* genomic DNA (JCM 20135, RIKEN BRC) using primer set 5′-

AAATTTATATTTTCAAGGATCCCATATGTTTTCAATGATATTAAG-3′ and 5′-GGCTTTGTTAGCAGCCCTCGAGTCAGGCTTTTTGAACGG-3′ (fig. S2A), and the *E. coli* MG1655 *ΔcysPUWA ΔyeeE::kan* (DE3) strain, which cannot grow on a minimum medium with thiosulfate ion as the single sulfur source (*6*). pAZ061 derivatives having mutations in the *yeeD* region were prepared by site-directed mutagenesis. The DNA sequence encoding YeeD was deleted from pAZ061 using primers 5′-GTTTGGGTTAGGCATCGCTTCCCCAACGGCC-3′ and 5′-GGCCGTTGGGGAAGCGATGCCTAACCCAAAC-3′.

The plasmid used to express *St*YeeE (1-328aa, UniProt ID: G0GAP6) with C-terminal GSSGENLYFQGEDVE-His_8 sequence (pKK550) was prepared as in (*6*). For the expression of the *St*YeeE-*St*YeeD fusion protein, we modified pKK550; the resulting plasmid, pAZ150, encodes *St*YeeE (1–330 aa)-AATPTPVAEAAPSSAEDRVLPFQVATGAVALQTAPRVKKA-*St*YeeD (1–80 aa, UniProt ID: G0GAP7)-GSSGENLYFQGEDVE-His_6. The mutations in the *St*YeeE and *St*YeeD regions were introduced by site-directed mutagenesis.

For the expression of *St*YeeD, the DNA sequence encoding *St*YeeD (1–80 aa) was inserted into a modified pCGFP-BC plasmid. The resulting plasmid, pNT015, expresses *St*YeeD (1–80 aa)-GSSGENLYFQGEDVE-His_6. The pNT015 derivatives were prepared by Gene Synthesis and Mutagenesis (SC1441, GenScript) or site-directed mutagenesis.

Growth complementation tests of *E. coli* cells

E. coli MG1655 *ΔcysPUWA ΔyeeE::kan* (DE3) cells harboring pAZ061 or its derivatives were cultured in LB medium containing 50 μg/ml ampicillin and 25 μg/ml kanamycin for 16 h at 37 °C. The culture was diluted 100-fold and cultured for another 8 h at 37 °C, after which the cells were precipitated by centrifugation and washed twice with S-free medium (42 mM Na_2HPO_4, 22 mM KH_2PO_4, 8.6 mM NaCl, 19 mM NH_4Cl, 1 mM $MgCl_2$, 0.2% (w/v) glucose, 0.01% (w/v) thiamine hydrochloride, and 0.1 mM $CaCl_2$). Subsequent passage cultures in S-free medium containing 500 μM $Na_2S_2O_3$ were started at OD_{600} = 0.2. The ΔOD_{600} of the culture was measured every 30 min with OD-Monitor C&T (TAITEC) for 24 h. Measurement was performed three times for each transformant.

Protein expression and purification

*St*YeeE and *St*YeeE(C22A)-YeeD proteins were purified as follows. *E. coli* C41(DE3) cells transformed with plasmids expressing these proteins were cultured in 2.5 l of LB medium containing 50 μg/ml ampicillin until the OD_{600} reached 0.4. Isopropyl β-D-thiogalactopyranoside (IPTG) was then added to 1 mM, and the cells were cultured at 30 °C for 17 h. Subsequent procedures were

317 performed at 4 °C or on ice. The cells were collected by centrifugation as pellets, suspended in a buffer
318 (10 mM Tris-HCl pH 8.0, 300 mM NaCl, 1 mM EDTA-Na pH 8.0, 2 mM $Na_2S_2O_3$, 0.1 mM
319 phenylmethylsulfonyl fluoride (PMSF), and 1 mM β–mercaptoethanol (β-ME)), and disrupted with a
320 Microfluidizer Processor M-110EH (Microfluidics International). The suspension was centrifuged
321 (10,000 rpm for 20 min, himac R13A rotor), and the collected supernatant was further ultracentrifuged
322 (40,000 rpm for 60 min, Beckman 45Ti rotor) to obtain the membrane fraction, which was flash-frozen
323 in liquid nitrogen and stored at -80 °C until purification. The membrane fraction was resuspended in
324 solubilization buffer (20 mM Tris-HCl pH 8.0, 300 mM NaCl, 2 mM $Na_2S_2O_3$, 10 mM imidazole-HCl
325 pH 8.0, 5% glycerol, 1 mM β-ME, 0.1 mM PMSF) containing 1% n-dodecyl β-maltoside (DDM) and
326 stirred at 4 °C for 60 min. The insoluble fraction was removed by ultracentrifugation (45,000 rpm for
327 30 min, Beckman 70Ti rotor), and the supernatant was mixed with 5 ml of Ni-NTA agarose (QIAGEN)
328 pre-equilibrated with solubilization buffer for 60 min. Then, 100 ml of wash buffer (20 mM Tris-HCl
329 pH 8.0, 300 mM NaCl, 2 mM $Na_2S_2O_3$, 50 mM imidazole-HCl pH 8.0, 5% glycerol, 1 mM β-ME, 0.1
330 mM PMSF, 0.1% DDM) was added to the column. Next, 5 ml of elution buffer (20 mM Tris-HCl pH
331 8.0, 300 mM NaCl, 2 mM $Na_2S_2O_3$, 200 mM imidazole-HCl pH 8.0, 5% glycerol, 1 mM β-ME, 0.1
332 mM PMSF, and 0.1% DDM) was added to the column six times, and the fractions with target proteins
333 were pooled. To remove the His-tag, TEV(S219V) protease (*24*) was added with a protein weight ratio
334 of 10 (proteins):1 (TEV) and the protein solution was dialyzed overnight against dialysis buffer (20
335 mM Tris-HCl pH 8.0, 300 mM NaCl, 2 mM $Na_2S_2O_3$, 0.1% DDM, 1 mM β-ME). Ni-NTA agarose
336 (2.5 ml) pre-equilibrated with dialysis buffer was added to the sample and stirred for 60 min to remove
337 TEV proteases. The flow-through fraction was collected, concentrated with an Amicon Ultra 50K
338 NMWL (Merck Millipore), and ultracentrifuged (45,000 rpm for 30 min, himac S55A2 rotor). The
339 sample was then applied to a Superdex 200 increase 10/300 GL column (Cytiva) equilibrated with a
340 buffer (20 mM Tris-HCl pH 8.0, 300 mM NaCl, 2 mM $Na_2S_2O_3$, 0.1% DDM, 1 mM β-ME). The
341 fractions with target proteins were collected and pooled. *St*YeeE(C22A)-YeeD(L45A) protein was
342 purified same as *St*YeeE and *St*YeeE(C22A)-YeeD except that the buffer without $Na_2S_2O_3$ was used.
343 *St*YeeD purification was performed as follows. *E. coli* C41(DE3) cells containing *St*YeeD-
344 encoding plasmids were inoculated into 25 ml of LB medium containing 50 μg/ml ampicillin and
345 cultured overnight at 37 °C. The culture was then added to 0.5 l of LB medium containing 50 μg/ml
346 ampicillin and allowed to grow until OD_{600} = 0.4. After the addition of IPTG to 1 mM, the cells were
347 cultured at 30 °C for 17 h. The cells were collected by centrifugation (4,500 rpm for 10 min, himac
348 R9A2), flash-frozen in liquid nitrogen, and stored at -80 °C until use. The next procedures were
349 performed at 4 °C or on ice. The frozen pellets were suspended in 25 ml of sonication buffer (20 mM

Tris-HCl pH 8.0, 300 mM NaCl, 10 mM imidazole-HCl pH 8.0, 1 mM β-ME, 0.1 mM PMSF), sonicated for 10 min on ice with a Q500 sonicator (QSONICA), and centrifuged (15,000 rpm for 30 min, himac R13A). Ni-NTA agarose (2.5 ml) pre-equilibrated with the sonication buffer was added to the supernatant and rotated for 1 h. After the flow-through fraction was removed, the resin was washed with 125 ml of a buffer (20 mM Tris-HCl pH 8.0, 300 mM NaCl, 20 mM imidazole-HCl pH 8.0, 1 mM β-ME, 0.1 mM PMSF). Next, 5 ml of a buffer (20 mM Tris-HCl pH 8.0, 300 mM NaCl, 200 mM imidazole-HCl pH 8.0, 1 mM β-ME, 0.1 mM PMSF) was added, and the elution fraction was collected. The elution step was repeated six times. The fractions with target proteins were pooled and concentrated using an Amicon Ultra 3K NMWL (Merck Millipore). The sample was ultracentrifuged (45,000 rpm x 30 min, himac S55A2 rotor) and loaded onto a Superdex 200 increase 10/300 GL column pre-equilibrated with YeeD gel filtration buffer (10 mM Tris-HCl pH 8.0 and 300 mM NaCl). The fractions with YeeD proteins were concentrated using an Amicon Ultra 3K NMWL.

MALDI-TOF MS

Purified *St*YeeD and *St*YeeD(C17A) in YeeD gel filtration buffer were used for mass spectrometry analysis. For the thiosulfate condition, *St*YeeD proteins (48.2 μM) were incubated with 300 mM thiosulfate at 37 °C for 2.5 h. For the DTT condition, *St*YeeD (48.2 μM) was incubated with 16.7 mM DTT at 37 °C for 10 min. After the reactions, the protein solutions were diluted 1,000 times with buffer (10 mM Tris-HCl pH 8.0) and concentrated using an Amicon Ultra 3K NMWL. StYeeD proteins (~80–120 μM) were analyzed by mass spectrometry. Samples for MALDI-TOF analysis were prepared by the sinapinic acid (SA) double layer method (*25*). In brief, 1 μl matrix solution A (saturated solution of SA in ethanol) was deposited onto the MALDI target and allowed to dry. Matrix solution B (saturated solution of SA in TA30 solvent (1:2 [v/v] acetonitrile:0.1% trifluoroacetic acid in water)) and protein solution were mixed at a ratio of 1:24 [v/v]. Matrix solution B/protein mixture was then deposited onto the matrix spot and allowed to dry. The dried samples were analyzed by Autoflex-II (Bruker Daltonics) with a linear positive mode and acquisition mass range of 3,000–20,000 Da. Theoretical m/z values were calculated with the equation of $m/z = (M + n)/n$, where M is molecular mass and n is the charge (n = 1 was adopted).

Measurement of enzyme activity of *St*YeeD

The release of H_2S due to chemical decomposition of thiosulfate ions by *St*YeeD was monitored by HSip-1 (Dojindo, SB21-10). The reaction solution contained 19.6 μM HSip-1, 24.1 μM YeeD, and 70 μM β-ME in the YeeD gel filtration buffer. As negative controls, 24.1 μM BSA was used instead of

YeeD, or no protein was added to the solution. The reaction was started by adding 5 µl of 100 mM $Na_2S_2O_3$ at a 1:200 [v/v] ratio (final, 500 µM $Na_2S_2O_3$), and the solution was incubated at 37 °C. The fluorescence of HSip-1 was measured using a fluorescence spectrophotometer (F-7000, Hitachi), at an excitation wavelength of 491 nm and an emission wavelength of 521 nm, every 30 min until 150 min.

Crystallization

Purified *St*YeeE(C22A)-*St*YeeD fusion protein was concentrated to 21.5 mg/ml by Amicon Ultra 50K NMWL and crystallized using the lipidic cubic phase (LCP) method, as previously performed in the case of purified YeeE (*6*). Fifteen microliters of 21.5 mg/ml *St*YeeE(C22A)-YeeD was mixed with 4.3 µl of a buffer (20 mM Tris-HCl pH 8.0, 300 mM $Na_2S_2O_3$, 0.1% DDM, 1 mM β-ME) and incubated on ice for 20 min. Then, 16 µl of the sample was mixed with 24 µl of monoolein (M-239, Funakoshi) in an LCP syringe (Art Robbins Instruments) for 10 min. After 30 min of incubation at 20°C, 30 nl of the mixed samples were spotted onto MRC under oil crystallization plates (Hampton Research) using the Crystal Gryphon protein crystallization aliquot system (Art Robbins Instruments) with 3 µl of buffers (18 to 24% pentaerythritol-propoxylate (5/4 PO/OH), 100 mM 2-morpholinoethanesulfonic acid (MES)-NaOH pH 7.0, and 300 mM NaCl) covering them. The plate was incubated at 20 °C for 7 days. For *St*YeeE(C22A)-YeeD(L45A) fusion protein, the purified protein was concentrated to 16.5 mg/ml and crystallized using the LCP method. The crystals appeared using 0.35 M ammonium formate, 0.1 M Tris-HCl (pH 8.0 to 9.0), and 22 to 42% 1,4-Butanediol as covering solutions. The plate was incubated at 20 °C for 14 days. The appeared crystals were harvested by Crystal Mounts and Loops (MiTegen), flash-frozen in liquid nitrogen, and stored in liquid nitrogen until X-ray diffraction experiments.

Data collection and structural determination

X-ray diffraction experiments of *St*YeeE(C22A)-*St*YeeD were performed at beamline BL32XU of SPring-8. Data were collected with the automated data collection system ZOO (*26*). The data were first processed with KAMO (*27*) using XDS (*28*). For *St*YeeE(C22A)-*St*YeeD dataset, the initial phase was determined by molecular replacement using the *St*YeeE crystal structure (PDB ID: 6LEO) as a template by PHASER (*29*), and a *St*YeeD structure predicted by AlphaFold2 (*15, 16*) was manually fitted to the density map using COOT (*30*). Structure refinement was performed using COOT (*30*) and PHENIX (*31*) iteratively until R_{work}/R_{free} reached 0.265/0.310 at 3.34 Å resolution. For *St*YeeE(C22A)-YeeD(L45A) dataset, the initial phase was determined by molecular replacement using

the *St*YeeE(C22A)-*St*YeeD structure as a template by MOLREP (*32*). Refinement of the structure was performed using COOT (*30*) and PHENIX (*31*) in a iterative way until R_{work}/R_{free} reached 0.206/0.255 at 2.60 Å resolution. Figures of the structures were prepared using PyMOL (https://pymol.org/2/) and Chimera (*33*).

Interaction analysis between *St*YeeE and *St*YeeD by the BLI method

BLI method (*21*) was performed to analyze the interaction between *St*YeeE and *St*YeeD-His_6 proteins using the Octet N1 System (Sartorius) at room temperature. A Ni-NTA biosensor was hydrated with Octet buffer (20 mM Tris-HCl pH 8.0, 300 mM NaCl, 0.1% DDM, 1 mM β-ME) for 10 min and mounted in the Octet N1 System. The biosensor was first dipped in Octet buffer, and the initial baseline was measured for 30 sec. Next, the biosensor was dipped in 4.82 μM *St*YeeD-His_6 protein solution in Octet buffer for 120 sec for loading. The solution was then changed to Octet buffer for 30 sec to measure the baseline, after which, the biosensor was submerged in 11.05 μM *St*YeeE solution in Octet buffer for 120 sec to measure the association of *St*YeeE. Finally, the buffer was exchanged to Octet buffer, and the dissociation of *St*YeeE from the biosensor was measured for 120 sec. Biosensors without *St*YeeD-His_6 proteins were measured with the same procedure and used as references. After the reference data were subtracted from *St*YeeD-His_6 protein data, the association rate constant (k_a), dissociation rate constant (k_d), and affinity constant (K_D) were calculated by a local fitting method. Measurements were performed three times for each protein.

Reconstitution of proteoliposomes

A mixture of 0.8 mg/ml *St*YeeE and 4 mg/ml *E. coli* total lipid extract (Avanti Polar Lipids) in a buffer (20 mM HEPES-HCl pH 7.0, 300 mM NaCl, 5% glycerol, and 0.1% DDM) was rotated at 4 °C for 1 h. Next, the detergent was removed using SM2-beads (Bio-Rad). The resulting solution was ultracentrifuged, and the precipitates were suspended in a buffer (25 mM HEPES-NaOH pH 7.5 and 100 mM NaCl). The reconstituted proteoliposome samples were flash-frozen in liquid nitrogen and stored at -80 °C until measurements.

Measurement of ion transport activity

The SSM method was used to detect thiosulfate uptake activity of the *St*YeeE-reconstituted proteoliposomes. Frozen proteoliposomes were thawed on ice and sonicated using a bath sonicator (VELVO-CLEAR, VS-50R) for 10 s three times before use. Measurement was performed using $SURFE^2R$ N1 (Nanion Technologies) as described (*14*). First, 50 μl of 0.5 mM 1-octadecanethiol

(dissolved in isopropanol) was applied to N1 Single Sensors (Nanion Technologies, Nr. 2-03-35002-000) and incubated for 30 min at room temperature. Next, the sensors were washed twice with isopropanol, washed twice with distilled water, and dried. Then, 1.5 µl of 7.5 µg/µl 1,2-diphytanoyl-sn-glycero-3-phosphocholin (dissolved in n-decane) was applied to the sensor, followed by 50 µl of non-activating buffer (B buffer: 140 mM NaCl, 4 mM $MgCl_2$, 25 mM HEPES, 25 mM MES, KOH pH 6.7, with or without Na_2SO_4). Proteoliposomes were pipetted toward the sensor beneath the B buffer surface, and the sensor was centrifuged (2,000*g* for 30 min, 25 °C) to adsorb the liposomes onto the sensor surface. The resultant sensors were mounted in SURFE^{2}R N1, and the sensors were rinsed with buffer B before each measurement. The current change on the sensor was monitored while B buffer and A buffer (140 mM NaCl, 4 mM $MgCl_2$, 25 mM HEPES, 25 mM MES, KOH pH 6.7, with $Na_2S_2O_3$) were exchanged. For each condition, measurement was performed four times, and the three results with least noise were analyzed.

REFERENCES AND NOTES

1. A. Francioso, A. Baseggio Conrado, L. Mosca, M. Fontana, Chemistry and Biochemistry of Sulfur Natural Compounds: Key Intermediates of Metabolism and Redox Biology. *Oxid Med Cell Longev* **2020**, 8294158 (2020).
2. G. D. Westrop, G. Goodall, J. C. Mottram, G. H. Coombs, Cysteine biosynthesis in Trichomonas vaginalis involves cysteine synthase utilizing O-phosphoserine. *J Biol Chem* **281**, 25062-25075 (2006).
3. T. Nakatani *et al.*, Enhancement of thioredoxin/glutaredoxin-mediated L-cysteine synthesis from S-sulfocysteine increases L-cysteine production in Escherichia coli. *Microb Cell Fact* **11**, 62 (2012).
4. C. T. Pereira, C. Roesler, J. N. Faria, M. R. Fessel, A. Balan, Sulfate-Binding Protein (Sbp) from Xanthomonas citri: Structure and Functional Insights. *Mol Plant Microbe Interact* **30**, 578-588 (2017).
5. A. Sirko, M. Hryniewicz, D. Hulanicka, A. Bock, Sulfate and thiosulfate transport in Escherichia coli K-12: nucleotide sequence and expression of the cysTWAM gene cluster. *J Bacteriol* **172**, 3351-3357 (1990).
6. Y. Tanaka *et al.*, Crystal structure of a YeeE/YedE family protein engaged in thiosulfate uptake. *Sci Adv* **6**, eaba7637 (2020).
7. B. K. Mohanty, S. R. Kushner, Inactivation of RNase P in Escherichia coli significantly changes post-transcriptional RNA metabolism. *Mol Microbiol* **117**, 121-142 (2022).

8. S. Morigasaki, A. Umeyama, Y. Kawano, Y. Aizawa, I. Ohtsu, Defect of RNA pyrophosphohydrolase RppH enhances fermentative production of L-cysteine in Escherichia coli. *J Gen Appl Microbiol* **66**, 307-314 (2021).

9. T. Yamashino, M. Isomura, C. Ueguchi, T. Mizuno, The yhhP gene encoding a small ubiquitous protein is fundamental for normal cell growth of Escherichia coli. *J Bacteriol* **180**, 2257-2261 (1998).

10. Y. Ikeuchi, N. Shigi, J. Kato, A. Nishimura, T. Suzuki, Mechanistic insights into sulfur relay by multiple sulfur mediators involved in thiouridine biosynthesis at tRNA wobble positions. *Mol Cell* **21**, 97-108 (2006).

11. J. U. Dahl *et al.*, The sulfur carrier protein TusA has a pleiotropic role in Escherichia coli that also affects molybdenum cofactor biosynthesis. *J Biol Chem* **288**, 5426-5442 (2013).

12. L. J. Liu *et al.*, Thiosulfate transfer mediated by DsrE/TusA homologs from acidothermophilic sulfur-oxidizing archaeon Metallosphaera cuprina. *J Biol Chem* **289**, 26949-26959 (2014).

13. T. S. Tanabe, S. Leimkuhler, C. Dahl, The functional diversity of the prokaryotic sulfur carrier protein TusA. *Adv Microb Physiol* **75**, 233-277 (2019).

14. A. Bazzone, M. Barthmes, K. Fendler, SSM-Based Electrophysiology for Transporter Research. *Methods Enzymol* **594**, 31-83 (2017).

15. M. Varadi *et al.*, AlphaFold Protein Structure Database: massively expanding the structural coverage of protein-sequence space with high-accuracy models. *Nucleic Acids Res* **50**, D439-D444 (2022).

16. J. Jumper *et al.*, Highly accurate protein structure prediction with AlphaFold. *Nature* **596**, 583-589 (2021).

17. E. Katoh *et al.*, High precision NMR structure of YhhP, a novel Escherichia coli protein implicated in cell division. *J Mol Biol* **304**, 219-229 (2000).

18. R. Shi *et al.*, Structural basis for Fe-S cluster assembly and tRNA thiolation mediated by IscS protein-protein interactions. *PLoS Biol* **8**, e1000354 (2010).

19. G. Tombline *et al.*, Pseudomonas aeruginosa PA1006 is a persulfide-modified protein that is critical for molybdenum homeostasis. *PLoS One* **8**, e55593 (2013).

20. E. Doka *et al.*, Control of protein function through oxidation and reduction of persulfidated states. *Sci Adv* **6**, eaax8358 (2020).

21. Y. Abdiche, D. Malashock, A. Pinkerton, J. Pons, Determining kinetics and affinities of protein interactions using a parallel real-time label-free biosensor, the Octet. *Anal Biochem* **377**, 209-217 (2008).

22. Y. Stockdreher *et al.*, New proteins involved in sulfur trafficking in the cytoplasm of Allochromatium vinosum. *J Biol Chem* **289**, 12390-12403 (2014).
23. Y. Daimon *et al.*, The TPR domain of BepA is required for productive interaction with substrate proteins and the beta-barrel assembly machinery complex. *Mol Microbiol* **106**, 760-776 (2017).
24. R. B. Kapust *et al.*, Tobacco etch virus protease: mechanism of autolysis and rational design of stable mutants with wild-type catalytic proficiency. *Protein Eng* **14**, 993-1000 (2001).
25. Y. Dai, R. M. Whittal, L. Li, Two-layer sample preparation: a method for MALDI-MS analysis of complex peptide and protein mixtures. *Anal Chem* **71**, 1087-1091 (1999).
26. K. Hirata *et al.*, ZOO: an automatic data-collection system for high-throughput structure analysis in protein microcrystallography. *Acta Crystallogr D Struct Biol* **75**, 138-150 (2019).
27. K. Yamashita, K. Hirata, M. Yamamoto, KAMO: towards automated data processing for microcrystals. *Acta Crystallogr D Struct Biol* **74**, 441-449 (2018).
28. W. Kabsch, Xds. *Acta Crystallogr D Biol Crystallogr* **66**, 125-132 (2010).
29. A. J. McCoy *et al.*, Phaser crystallographic software. *J Appl Crystallogr* **40**, 658-674 (2007).
30. P. Emsley, B. Lohkamp, W. G. Scott, K. Cowtan, Features and development of Coot. *Acta Crystallogr D Biol Crystallogr* **66**, 486-501 (2010).
31. P. V. Afonine *et al.*, Towards automated crystallographic structure refinement with phenix.refine. *Acta Crystallogr D Biol Crystallogr* **68**, 352-367 (2012).
32. A. Vagin, A. Teplyakov, Molecular replacement with MOLREP. *Acta Crystallogr D Biol Crystallogr* **66**, 22-25 (2010).
33. E. F. Pettersen *et al.*, UCSF Chimera--a visualization system for exploratory research and analysis. *J Comput Chem* **25**, 1605-1612 (2004).
34. X. Robert, P. Gouet, Deciphering key features in protein structures with the new ENDscript server. *Nucleic Acids Res* **42**, W320-324 (2014).

Acknowledgments: We thank Kayo Abe for secretarial assistance, Akira Sasaki for liposome preparation, Rie Kurata for performing mass spectrometry, Naoki Sakai for helping with the data analysis, the beamline scientists at BL32XU of SPring-8 (Hyogo, Japan) for helping with data collection, and Nanion Technologies for assistance with initial data collection. The synchrotron radiation experiments were performed at BL32XU of SPring-8 with the approval of the Japan Synchrotron Radiation Research Institute (JASRI) (Proposal Nos. 2020A2564, 2021A2745). **Funding:** This work was supported by JSPS/MEXT KAKENHI (Grant Nos. JP22K15075, JP20K15733 to M. Ichikawa, Grant No. JP22K15061, JP22H05567 to R.M., and Grant Nos.

JP22H02567, JP22H02586, JP21H05155, JP21H05153, JP21K19226, JP21KK0125 to T.T.), PRESTO (JPMJPR20E1 to M. Ichikawa) from the Japan Science and Technology Agency (JST), and private research foundations (the Chemo-Sero-Therapeutic Research Institute, Naito Foundation, Takeda Science Foundation, G-7 Scholarship Foundation, the Sumitomo Foundation, the Institute for Fermentation (Osaka), Yamada Science Foundation, and Japan Foundation for Applied Enzymology) to T.T. *E. coli* JCM20135 was provided by RIKEN BRC, which is participating in the National Bio-Resources Project of MEXT, Japan. **Author Contributions:** Conceptualization, A.T., M. Ichikawa, and T.T.; Methodology and investigation, M. Ikei, R.M., K.M., Y.N., A.T., Y.S.T., Y.T., T.M., M. Ichikawa, and T.T.; Writing – original draft, M. Ichikawa and T.T.; Writing, review & editing, M. Ichikawa and T.T.; Supervision, M. Ichikawa and T.T. **Competing interests:** The authors declare no competing interests. **Data and materials availability:** Coordinates and structure factors have been deposited in the Protein Data Bank under accession number 8J4C and 8K1R. All data needed to evaluate the conclusions in the paper are present in the paper and/or the Supplementary Materials. Additional data related to this paper may be requested from the authors.

FIGURES AND TABLES

Table 1. Data collection and refinement

Statistics for the highest-resolution shell are shown in parentheses.

PDB ID	8J4C	8K1R
Data Collection		
X-ray source	SPring-8 BL32XU	SPring-8 BL32XU
Wavelength (Å)	1.00	1.00
Space group	$P2_122_1$	$P2_122_1$
a, b, c (Å)	73.98, 102.44, 186.52	73.58, 101.75, 182.76
Resolution range (Å)	47.60–3.34 (3.46–3.34)	49.01–2.60 (2.69–2.60)
Total reflections	432750 (38159)	13803448 (1256177)
Unique reflections	21249 (2011)	42977 (4206)
Multiplicity	20.4 (18.4)	321.2 (297.1)
Completeness (%)	99.04 (96.87)	99.52 (99.32)
$I/\sigma(I)$	4.12 (0.83)	15.25 (2.10)
Wilson B-factor	49.19	31.95
R-pim	0.2207 (1.017)	0.0478 (0.2706)
$CC_{1/2}$	0.963 (0.578)	0.996 (0.861)
Refinement		
Reflections used in refinement	21070 (2011)	42846 (4206)
Reflections used for R-free	1990 (190)	1993 (196)
R_{work}	0.2654 (0.3596)	0.2064 (0.2705)
R_{free}	0.3095 (0.4113)	0.2547 (0.3108)
Number of non-	6675	6900
Protein	6238	6247
Ligand	437	545
RMS derivations		
bond length (Å)	0.003	0.009
bond angles (°)	0.56	1.16
Ramachandran		
favoured (%)	94.80	96.77
allowed (%)	4.95	2.73
outliers (%)	0.25	0.50
Average B-factor	66.46	39.54
Protein	67.97	38.61
Ligand	44.86	51.12

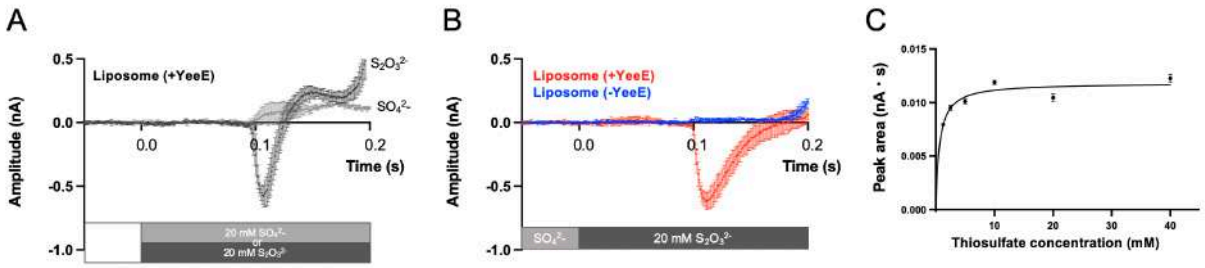

Fig. 1. Thiosulfate ion transport activity of *St*YeeE-reconstituted liposomes.

(**A**) Selective uptake of thiosulfate ion by *St*YeeE. *St*YeeE-reconstituted liposomes were used for the measurement using the SSM method. The non-activation buffer, lacking any sulfur-related ions, was exchanged with buffer containing either 20 mM $Na_2S_2O_3$ or 20 mM Na_2SO_4 at 0.0 s. (**B**) YeeE-dependent negative current changes. Liposomes with and without *St*YeeE were used. The non-activation buffer containing 20 mM Na_2SO_4 was exchanged with buffer containing 20 mM $Na_2S_2O_3$ instead of Na_2SO_4 at 0.0 s. The current values from three measurements were standardized based on the average values from -0.05 to 0.0 s, and then the mean values from the three measurements were calculated. Error bars indicate the SD (standard deviation). (**C**) Thiosulfate concentration dependency of the uptake activity. The current changes were monitored in the same manner as in (B), except for the concentration of thiosulfate and sulfate ions (1.25, 2.5, 5, 10, 20, and 40 mM). The negative peak area values (nA・s) from three measurements were calculated and plotted with the SD. The plot was fitted with Michaelis–Menten equation, and V_{max} was estimated as 0.01184 nA・s and K_m as 0.6261 mM.

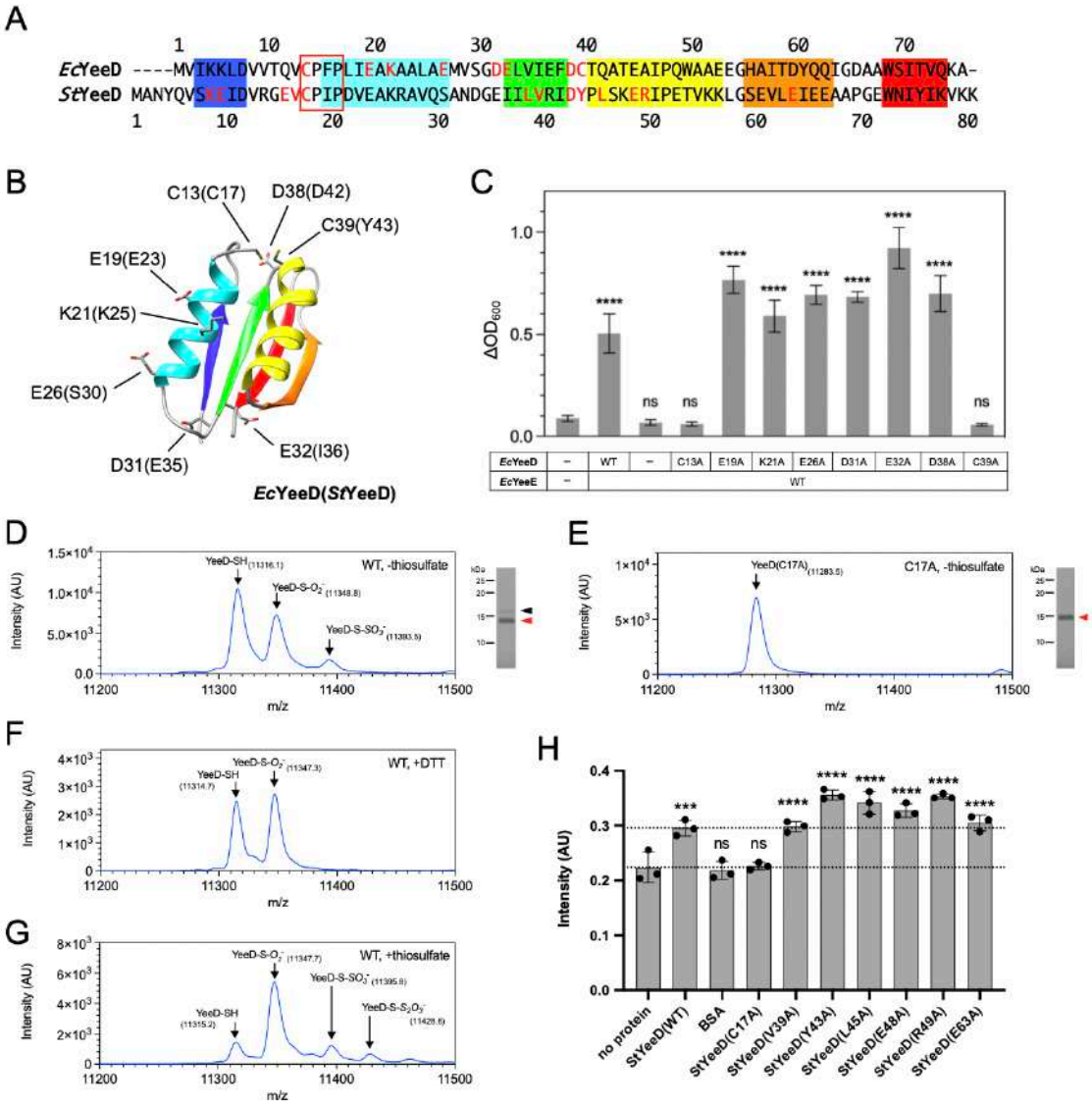

Fig. 2. Characterization of YeeD functions in vivo and in vitro.

(**A**) Sequence alignment of *Ec*YeeD and *St*YeeD. The regions of α-helices and β-strands predicted by AlphaFold2 in (B) are highlighted with colors. Red text indicates amino acid residues that were mutated in this study. The conserved CPxP motif is enclosed in a red rectangle. (**B**) Cartoon model of AlphaFold2-predicted structure of *Ec*YeeD. α-helices and β-strands are colored as in (A). The side chains of amino acid residues mutated for growth complementation analysis in (C) are shown as stick models. Corresponding amino acid residues from *St*YeeD are also indicated in parentheses. (**C**) Growth complementation assay of Δ*cysPUWA* Δ*yeeE* (DE3) cells, depending on *Ec*YeeE and *Ec*YeeD expression from plasmids. The mean values of increased OD_{600} (ΔOD_{600}) after 24 h are shown. Error bars represent the SD from three measurements. Statistical significance compared with the Δ*cysPUWA* Δ*yeeE* (DE3) cells possessing an empty vector was determined using one-way analysis of variance

(ANOVA) followed by Dunnett's multiple comparisons tests (****, $p < 0.0001$; ns, not significant). (**D**) CBB-stained SDS-PAGE gel and mass spectrometry of purified *St*YeeD (WT). Red and black arrowheads indicate the major and minor bands of purified WT *St*YeeD, respectively. In mass spectrometry, three major peaks corresponding to -SH, -S-O_2^-, and -S-SO_3^- were detected. (**E**) CBB-stained SDS-PAGE gel and mass spectrometry of purified *St*YeeD(C17A). In mass spectrometry, a single peak was observed. (**F** and **G)** Mass spectrometry of purified *St*YeeD (WT) in the presence of DTT (F) and thiosulfate ion (G). (**H**) Measurement of in vitro enzymatic activity of *St*YeeD. Fluorescence intensity changes derived from an H_2S-detectable fluorescent probe, HSip-1, in the presence of thiosulfate were measured using a series of purified *St*YeeD derivatives. Mean values of three experiments are shown. Error bars represent SD. Statistical significance compared with samples containing no protein was determined using one-way ANOVA followed by Dunnett's multiple comparisons tests (***, $p < 0.001$; ****, $p < 0.0001$; ns, not significant). Dashed lines indicate the mean values of no-protein samples and *St*YeeD(WT).

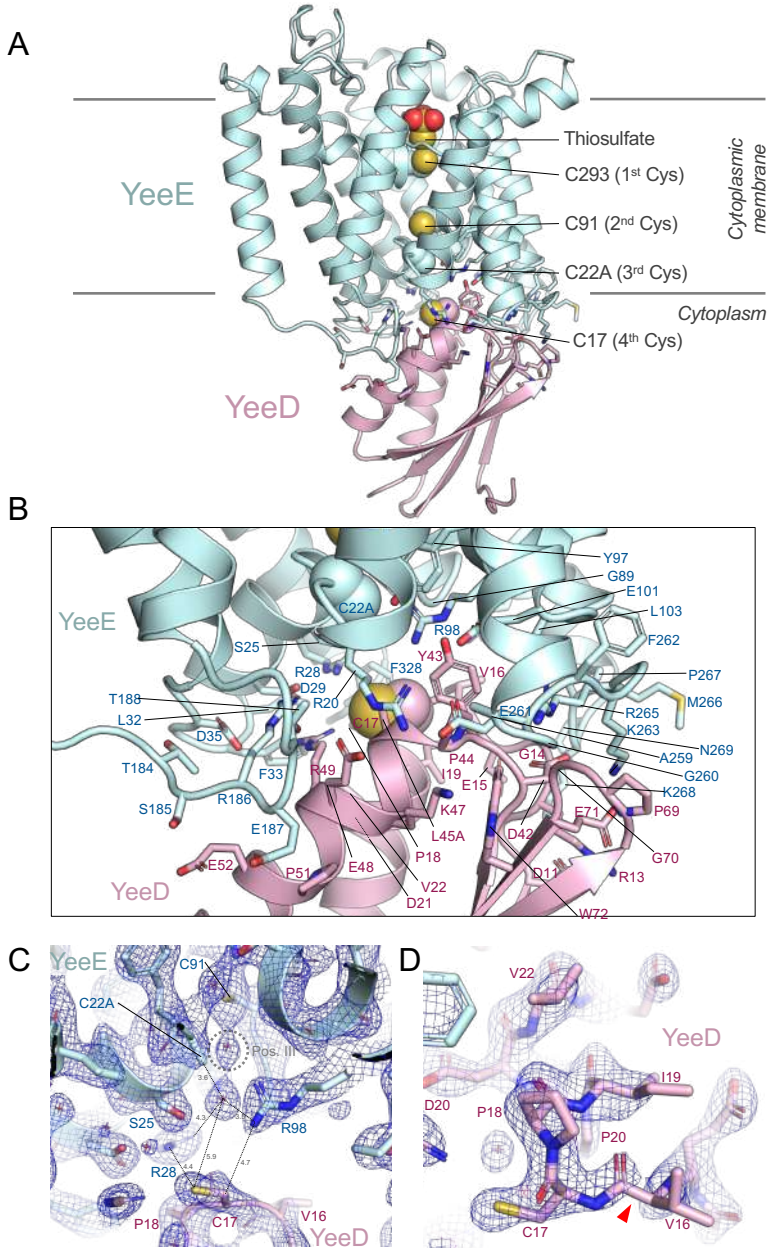

631

632 **Fig. 3. Crystal structure of YeeE-YeeD complex.**

633 (A) Cartoon model of YeeE(C22A)-YeeD(L45A). The side chains of amino acid residues on the
634 contact surfaces between YeeE and YeeD are shown as stick models. The side chains of the conserved
635 cysteine positions are shown in the spheres model. The thiosulfate ion in YeeE(C22A)-YeeD model in
636 the spheres model was superimposed. (**B**) Close-up view of the contact region. (**C**) 2Fo-Fc electron
637 density map at 1.5 δ of the border region around C22A in YeeE and C17 in YeeD. Position III is a
638 previously proposed thiosulfate-binding site. The red stars indicate water molecules. (**D**) 2Fo-Fc
639 electron density map at 1.3 δ around the CPxP motif. The red arrowhead indicates where the electronic
640 map is faint.

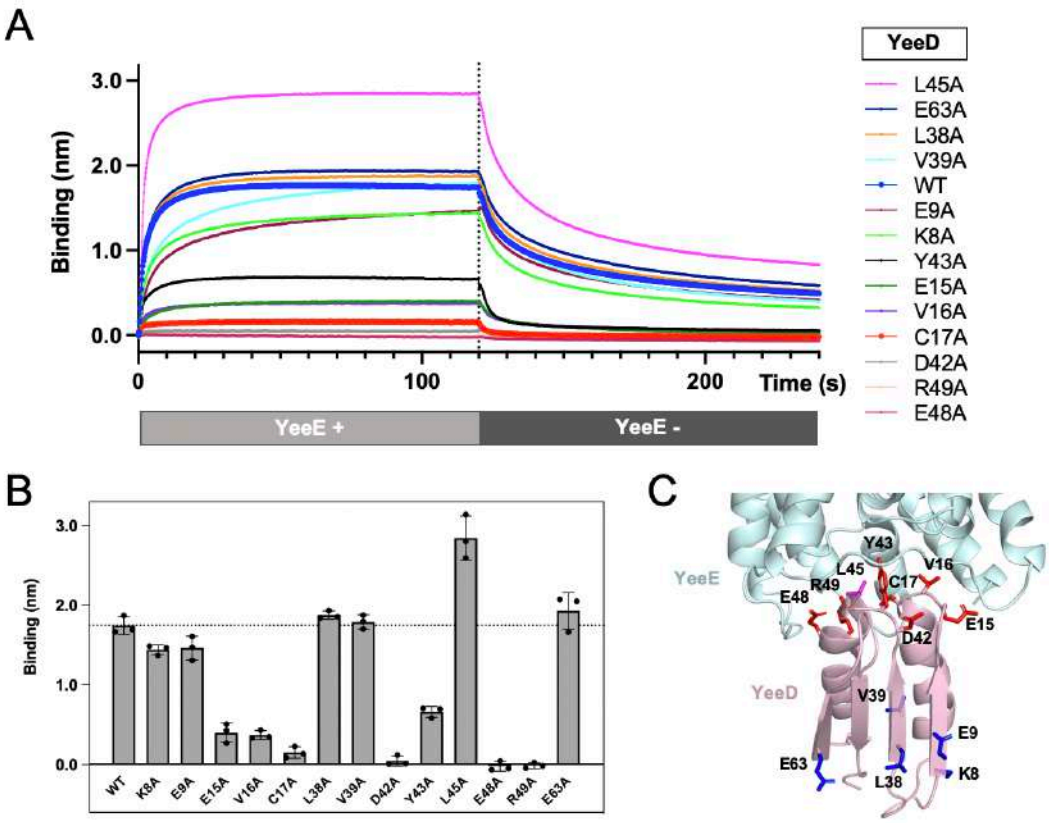

Fig. 4. Interaction between YeeE and YeeD.

(**A**) Real-time detection by the BLI method of association and dissociation of YeeE with/from solidified YeeD and its derivatives. Each line shows the mean value of three measurements. The dashed line indicates the 120-s point where YeeD-solidified biosensors were submerged in the YeeE-free buffer. (**B**) Mean values of YeeE binding to solidified YeeD at 120 s. Error bars show the SD of three measurements. The dashed line indicates the mean value of YeeD(WT). (**C**) Mutation site mapping on the crystal structure of the YeeE-YeeD complex. The side chains of mutated amino acid residues in (A) are shown as stick models. Magenta, blue, and red residues indicate that those Ala-substituted mutants showed increased, similar, and reduced binding affinity, respectively, compared to WT.

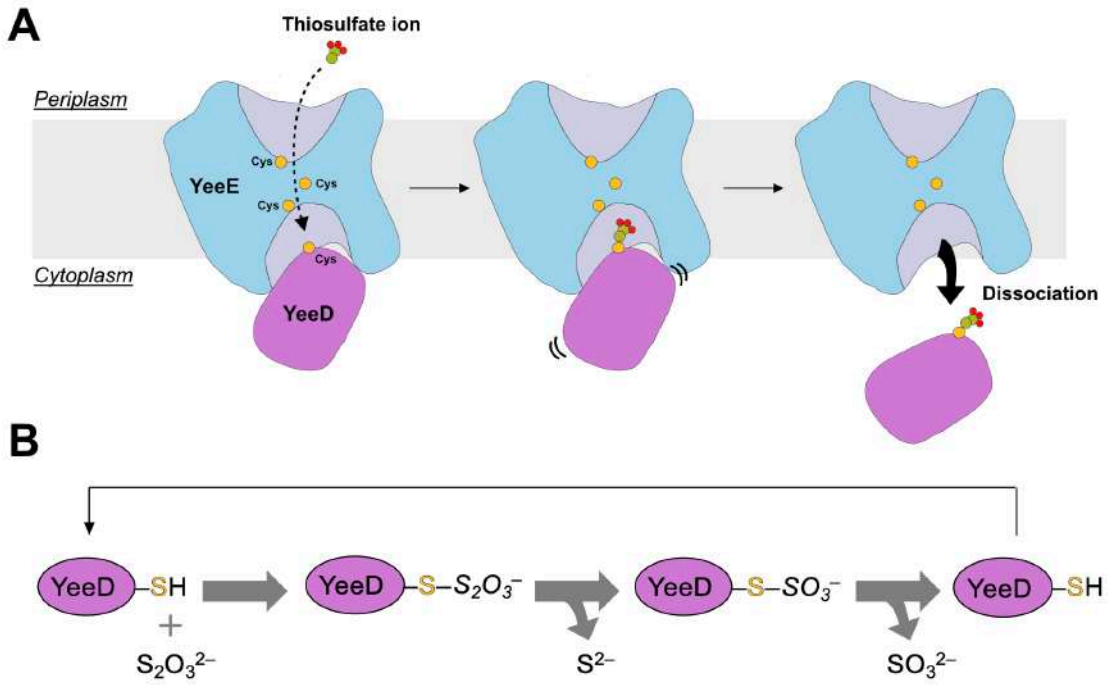

Fig. 5. Model of uptake and decomposition of thiosulfate ion by YeeE and YeeD.

(**A**) Uptake of a thiosulfate ion by YeeE and YeeD. The thiosulfate ion is relayed by conserved cysteine residues of YeeE and binds to the conserved cysteine residue of YeeD. After that, the association of YeeD with YeeE is destabilized. YeeD then dissociates from YeeE and decomposes the thiosulfate. (**B**) Thiosulfate decomposition by YeeD. First, thiosulfate binds directly to the conserved cysteine residue of YeeD. Next, sulfide ion (S^{2-}) is released. Finally, sulfite ion (SO_3^{2-}) is released.